Energetics of normal earthquakes on dip-slip faults

David Dempsey[1], Susan Ellis[2], Rosalind Archer[1], and Julie Rowland[3]
[1]Department of Engineering Science, University of Auckland, Private Bag 92019, Auckland Mail Centre, Auckland, New Zealand
[2]GNS Science, 1 Fairway Drive, Lower Hutt, New Zealand
[3]School of Environment, University of Auckland, Private Bag 92019, Auckland Mail Centre, Auckland, New Zealand

ABSTRACT

That earthquakes release vast quantities of energy is widely accepted; however, the most commonly experienced component, radiated seismic energy, is a minor contribution to the total energy budget. The elastic rebound model for earthquakes recognizes that elastic strain energy does work displacing, deforming, and accelerating the crust, as well as causing frictional heating. In this paper we present an energy budget for dip-slip fault rupture in an extensional tectonic regime. A computational model of an elastic-plastic-viscous crust hosting a single fault, modeled as two surfaces in frictional contact, demonstrates contrasting energy flows between the hanging-wall and footwall fault blocks. Our analysis suggests that in the period leading up to an earthquake, the total strain energy contained within the crust decreases, although a local increase within the footwall at mid-crustal depths is observed. During an earthquake, the footwall is subject to an elastic rebound, whereupon uplift of the fault scarp is caused by a mid-crustal stress drop and elastic expansion that releases strain energy. In contrast, gravitational potential energy released from a subsiding hanging wall does work compressing the wider crust, particularly in the mid-crust at the fault tip. This has the unusual consequence of increasing strain energy throughout much of the upper crust during an earthquake. These counterintuitive energy flows suggest that extensional deformation is caused by stored gravitational potential and elastic strain energy, and not by the external tectonic forcing.

BACKGROUND

The conventional view of earthquakes asserts that elastic strain energy (Reid, 1911; Sibson, 1974) accumulates within the crust during an interseismic period of fault dormancy prior to its release through fault rupture. This description of the seismic cycle implies that work done by tectonic forces stores elastic energy (EE), which in turn is expended to do work accelerating and deforming the crust during an earthquake via elastic rebound. The elastic rebound model was developed for strike-slip systems (Reid, 1911), where gravitational forces do not contribute to the work budget. However, geodetic observations of normal earthquakes on dip-slip faults record a significant drop in elevation of the hanging wall (e.g., Barrientos et al., 1987; Koukouvelas and Doutsos, 1996), which implicates gravitational potential energy (GPE) as a contributor to coseismic deformation in extensional tectonic environments (e.g., McKenzie, 1978; Stewart, 1980).

Recent examinations of the energy budget for thrust fault systems (Cooke and Murphy, 2004; Del Castello and Cooke, 2007) indicate a response consistent with elastic rebound, i.e., elastic strain energy is expended to do work against friction on the fault and against gravity deforming the surface, with a smaller component of radiated seismic energy. Here we consider an energy budget derived from a two-dimensional (2-D) computational model of a dip-slip fault within an extending elastic-plastic-viscous crust. Our analysis contrasts the ability of stored EE and GPE to do work against friction and gravity (Tanimoto et al., 2002) and to cause brittle or ductile deformation during the seismic cycle. Radiated seismic energy, which is a minor component of the work of faulting at low seismic efficiencies (e.g., McGarr, 1994; Kanamori, 2001), is not accounted for in the static analysis presented.

MODEL DESCRIPTION

Following Ellis et al. (2006), a 2-D crust, 60 km wide and 25 km deep (Fig. 1A), is modeled under plane-strain conditions using the finite element software Abaqus/Standard (http://www.simulia.com/products/abaqus_standard.html). Boundary-parallel free-slip boundary conditions are applied at the base and sides of the model while the top surface is free to deform. Extension of 12 mm yr^{-1} is divided equally between the two lateral boundaries and a linear temperature gradient of 35 °C km^{-1} is imposed throughout the crust.

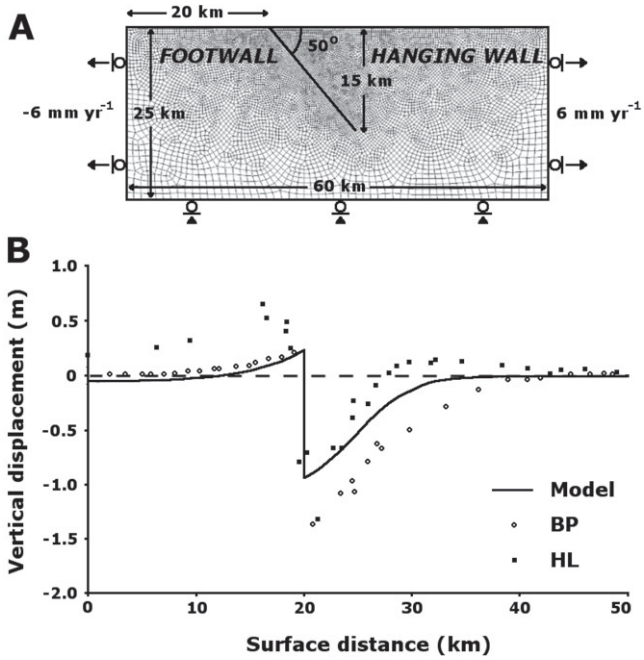

Figure 1. A: Model dimensions and boundary conditions applied during stress spin-up phase and seismic cycling, superimposed on model mesh. We used ~10,000 elements ranging in size from 1000 m at the base to 250 m on the fault. B: Coseismic vertical surface displacements produced by model (solid line) and for historical earthquakes at Borah Peak (BP), Idaho (1983, *M* = 6.9), and Hegben Lake (HL), Montana (1959, *M* = 7.3). Note that error bars for historical data are smaller than marker dimension.

Deformation of the crust is governed by linear, isotropic elasticity, limited by frictional plastic Mohr-Coulomb yield giving way to thermally controlled power-law creep with increasing depth. Frictional yield incorporates a modified strength to account for effects of hydrostatic pore fluid pressure (Byerlee, 1978; Townend and Zoback, 2000). The transition to power-law dislocation creep is determined by the model for ambient temperatures, pressures, and strain rates; we delineate upper and lower regions of the crust based on the depth to the brittle-ductile transition, which occurs at temperatures >~350 °C for the imposed bulk strain rate of 6×10^{-15} s^{-1} (see the GSA Data Repository[1]).

The crust hosts a single fault, modeled as two surfaces in frictional contact (e.g., Ellis et al., 2006; Nüchter and Ellis, 2010), dipping at 50° to a depth of 15 km. The seismic cycle is approximated by a 250 yr period of

[1]GSA Data Repository item 2012068, Table DR1, summary of model methods and rheologies, is available online at www.geosociety.org/pubs/ft2012.htm, or on request from editing@geosociety.org or Documents Secretary, GSA, P.O. Box 9140, Boulder, CO 80301, USA.

dormancy, in which fault creep is prohibited by an infinite friction coefficient along the fault plane. The static effects of an earthquake are simulated by changing the friction coefficient to a slip-weakened value of 0.2 (e.g., Scholz and Engelder, 1976) for a 60 s period. Note that dynamic effects such as wave propagation and rate-state friction are neglected, which precludes estimation of brittle afterslip or radiated seismic energy. The stress state is "spun-up" (e.g., Ellis et al., 2006; Hetland and Hager, 2006) over multiple earthquake cycles. Self-similar patterns of stress and deformation emerge after 10 cycles, indicating that a state of dynamic equilibrium has been achieved, and energy results presented are derived after the 12th cycle.

The model produces coseismic vertical surface displacements (Fig. 1B) that are qualitatively similar to geodetic observations following the M_w = 6.9 1983 Borah Peak earthquake (Idaho, USA) and the M_w = 7.3 1959 Hegben Lake earthquake (Montana, USA) (Barrientos et al., 1987). Both historical earthquakes exhibit well-resolved vertical displacement profiles and are inferred to have occurred on fault planes dipping at 50°. Comparison between these profiles shows that the model reproduces uplift of the footwall block and collapse of the adjacent hanging wall, with a total vertical offset at the surface of 1.2 m. For a 25-km-long surface rupture, this offset corresponds to an M = 5.8 earthquake (Hanks and Kanamori, 1979). Magnitudes and offsets for the historical earthquakes are larger than that in the model, which suggests either a greater stress buildup before rupture for those faults, or some difference in the elastic properties of the crust, e.g., Young's modulus (Gudmundsson, 2004). The comparatively smaller fault ruptures modeled here indicate that unrealistically large stress states are not attained.

EXTENSION, STRESS, AND STRAIN ENERGY

A consequence of lithostatic loading is that, with the exception of the near surface in extensional regimes, normal stresses within the crust are always compressive. Thus, a volume of rock brought to the surface from depth expands in response to the removal of lithostatic forces. Such physics underpin the violent and rapid expansion of rock associated with wellbore breakout (Zoback et al., 1985) and rock-burst phenomena (e.g., Cook et al., 1966). It also attests to the vast reservoirs of EE that exist within the crust and are accessible via changes in the stress state.

Adopting the convention that stresses and strains are positive in compression, we consider a crustal volume in which a small increment of tectonic extension occurs. This extension is associated with a small, negative change in horizontal stress. As the existing horizontal stress state is compressive, and thus positive, the addition of a negative stress change moves the crust incrementally closer to zero stress. The corresponding changes in elastic strain, and thus elastic strain energy, are then negative. The reduction of internal energy indicates that work has been done by, not on, the crustal volume, and implies that extension might be caused by the crust, rather than imposed by some external force. The validity of these concepts is tested in the next section by considering energy flows within a faulted crust undergoing extension.

ENERGY CONSERVATION AND WORK BALANCE

A static energy budget (e.g., Cooke and Murphy, 2004; Savage and Cooke, 2010) for the model is composed of strain energy (EE), energy dissipated by viscous (VE) or frictional plastic (PE) means, energy dissipated by frictional slip along the fault surface (FE), and work done on the model by external forces (W). External work includes work against gravity (thus W includes changes in GPE) and work done by tractions at the model boundaries. Strain energy, EE, is further decomposed into volumetric, EE_{VOL}, and distortional, EE_{DIS}, components, representing energy flow due to changes in volume and shape, respectively. Conservation of energy for the systems is then expressed as W = EE + VE + PE + FE. Details of the calculation of these energy terms can be found in Cooke and Murphy (2004) and Popov and Sobolev (2008).

Figure 2A presents the evolution of each energy budget component summed over the model domain over several seismic cycles from a common origin. Energy dissipation terms, i.e., PE, VE, and FE, plot in the positive domain and are always increasing due to their irreversible nature. Due to its recoverable nature, EE is permitted to plot in either domain.

The application of far-field tectonic forces over many seismic cycles evolves an extensional deviatoric stress, i.e., $\sigma_x < \sigma_z$ and $\sigma_x, \sigma_z > 0$, such that the continuous accumulation of horizontal elastic strain is limited by the Mohr-Coulomb yield criterion. Deformation post-yield, termed frictional plastic, corresponds physically to slip on preexisting fracture planes accompanied by the dissipation of EE as heat. This energy dissipation is widespread and consistent in time, except for a brief postseismic period (PE in Fig. 2A), in which the upper crustal stress state is below yield. The reduction in the rate of accumulation of PE is due to a coseismic increase in horizontal compression, which suppresses failure. This effect is reversed by continued tectonic extension following an earthquake.

Viscous deformation in the lower crust dissipates deviatoric stresses, and thus EE_{DIS}, that are generated by extension. This occurs at an almost constant rate that is insensitive to the earthquake cycle. Combined with the frictional plastic deformation that operates in the upper crust, these mechanisms ensure that the EE profile trends downward during the interseismic period. Summing PE, VE, and EE components during the interseismic period produces the external work profile, W, and its decline indicates that work is being done by, not on, the crust between earthquakes. In contrast, models of thrust faulting (Del Castello and Cooke, 2007; Cruz et al., 2010) demonstrate that external work is done on the crust in these systems.

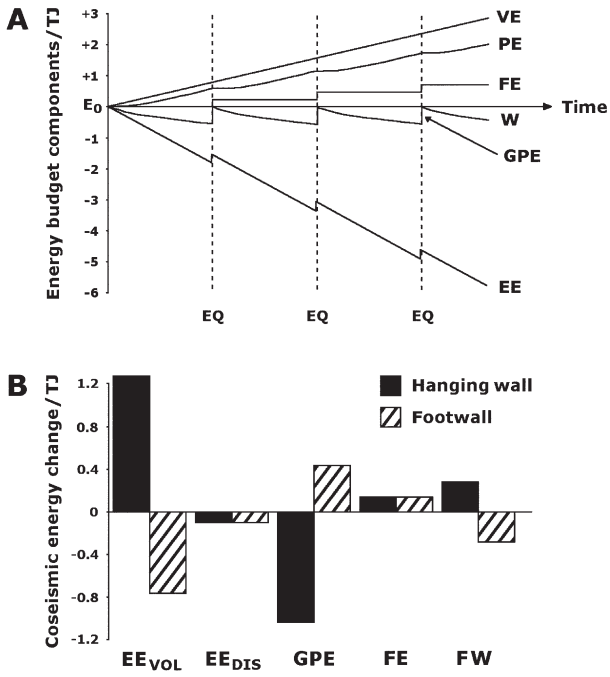

Figure 2. Energy budget during seismic cycle. A: Evolution over several seismic cycles of energy budget components, i.e., W = EE + PE + VE + FE, relative to their initial values, E_o, and summed over model domain. VE = energy dissipated by viscous strain; PE = energy dissipated by frictional plastic strain; FE = energy dissipated by frictional slip along fault; W = work done by external forces including gravity and tractions at boundaries; EE = changes in elastic energy. Note that W includes changes in gravitational potential energy (GPE) as indicated for final coseismic period. Earthquakes (EQ) are marked by dashed lines. B: Coseismic energy changes within hanging wall (solid) and footwall (hachured) blocks. Note that EE has been divided into volumetric, EE_{VOL}, and distortional, EE_{DIS}, components.

Relative to the interseismic period, an earthquake is a brief event during which boundary displacements are negligible. Any change in W then represents work done by gravity alone, i.e., a negative change in GPE. During an earthquake energy flow is limited to a decrease in GPE, and increases in EE and FE (Fig. 2A), as frictional plastic and viscous deformation operate too slowly to have an appreciable effect. These changes are an aggregate of three concurrent processes: a localized reduction in stress in the mid-crust that does work against friction and gravity to uplift the footwall; gravitational collapse of the hanging wall, which compresses the mid-crust and creates EE; and widespread horizontal compression of the upper crust, which creates EE and temporarily suppresses frictional plastic deformation. While the final two processes differ in scale only, their consequent effects on surficial processes warrant distinction.

Coseismic components of the energy budget are resolved within each fault block by extending the fault plane to the base of the model and summing components on either side. Changes in these components (Fig. 2B) indicate that mechanisms of deformation differ across the fault plane. For example, energy flow within the footwall is characteristic of an elastic rebound; 0.85 TJ of EE are expended to produce 0.43 TJ of GPE, manifesting as surface uplift, and 0.14 TJ frictional heating along the fault. The EE expended is mostly volumetric with a small distortional component, and represents a reduction in stress that drives an expansion of the mid-crust and vertical movement of the footwall. The remaining EE_{VOL}, ~0.28 TJ, is used to do work on the hanging-wall block, resulting in a normal displacement of the fault plane of as much as 20 cm at mid-crustal depths. This work, termed FW, is internal and not encapsulated by W in Figure 2A.

Energy changes within the hanging wall attest to a contrasting mechanism of deformation. In this block 1.0 TJ of GPE, 0.1 TJ of distortional elastic energy, i.e., EE_{DIS}, and 0.28 TJ of internal work done by the footwall, i.e., FW, is converted to 1.3 TJ of EE_{VOL} and 0.14 TJ of frictional heating along the fault. In physical terms, the GPE reduction that occurs due to a loss of elevation is used to do work to compress the crust, thereby creating EE. Work done to cause this compression is derived primarily from a loss of GPE rather than an elastic bounce-back of the fault block. In this sense the elastic response of the hanging wall differs fundamentally from that of the footwall.

ENERGY FLOW DURING THE SEISMIC CYCLE

Further insight into footwall elastic rebound and hanging-wall collapse is gained by identifying those regions from which energy is given up and to which energy flows. Dissipation of heat by fault friction and internal work (FE and FW in Fig. 2B) are both restricted to the fault plane; however, changes in EE_{VOL}, EE_{DIS}, and GPE occur throughout the crust.

Distortional changes in strain energy are consistent with the elastic rebound interpretation, i.e., EE_{DIS} accumulates in the upper crust (shallower than 8 km) during the interseismic period, and is subsequently released during fault rupture (Fig. 3A). A particularly large release of EE_{DIS} occurs within the footwall close to the fault plane and is associated with up-dip displacement of the fault block. Concurrently the near-fault region at mid-crustal depths (8–12 km) undergoes an increase in EE_{DIS}, principally within the hanging wall. This is associated with an increase in stress at the maximum gradient in fault slip (inset, Fig. 3A). This anomaly is largely dissipated by viscous deformation in the interseismic quiescence following an earthquake (Ellis et al., 2006).

Changes in EE_{VOL} and GPE are approximately an order of magnitude greater than EE_{DIS} and are thus primary drivers of coseismic deformation. At a depth of 8–10 km in the footwall there is a large decrease in EE_{VOL}, representing a rapid decrease in mid-crustal stress and associated expansion of the crust. This energy, which had accumulated in the preceding interseismic period, does work against gravity, resulting in uplift of the footwall (Fig. 1B) and the creation of GPE (Fig. 3C). Vectors of displacement direction show that footwall uplift occurs in the wider context of block rotation.

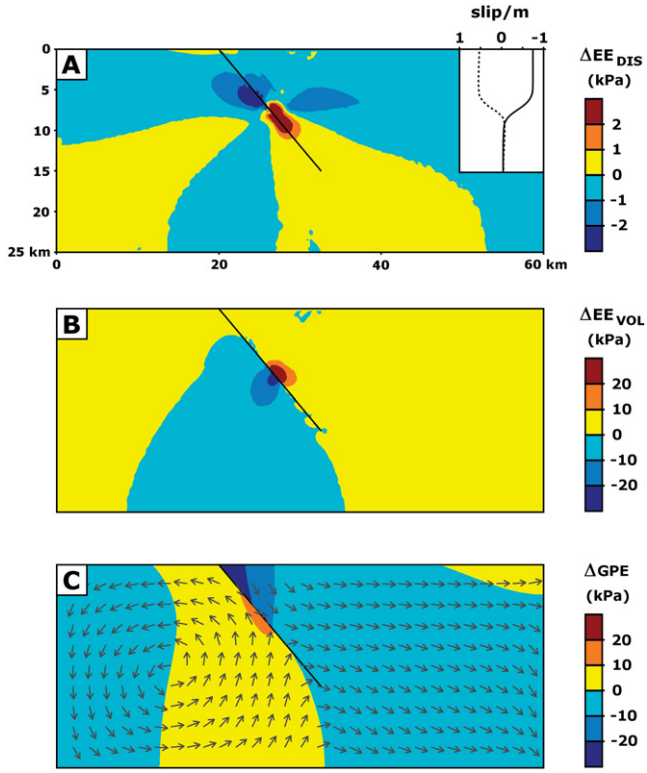

Figure 3. Contours of coseismic change in energy density throughout crust. A: Elastic energy, EE_{DIS} (distortional). B: EE_{VOL} (volumetric). C: Gravitational potential energy (GPE). Vectors on C indicate displacement direction. Contour levels for A are order of magnitude smaller than B and C, and units for energy density are dimensionally equivalent to stress. As model is in dynamic equilibrium, changes in EE_{DIS} and EE_{VOL} during interseismic period are equal in distribution but opposite in sign to those in A and B, respectively. Dip-slip profiles for footwall (dotted) and hanging wall (solid) are inset in A. Vertical scale is same as contour plot and down-dip slip is negative.

In the hanging wall, coseismic displacement is down dip or directed horizontally away from the fault. The crust immediately adjacent to the fault subsides by as much as 1 m at the surface (Fig. 1B), and a reduction in GPE from this region is observed (Fig. 3C). A concurrent increase in EE_{VOL} occurs at depths of 6–10 km corresponding to the cessation of slip on the fault plane.

In addition to these localized elastic changes, there is also a widespread, low-level increase in EE_{VOL} throughout the majority of the upper crust. This increase is ~50% larger than the simultaneous reduction in EE_{DIS} (Fig. 3A), and thus the net change in EE is positive during an earthquake. The increase in EE_{VOL} is due to horizontal compression of the crust as fault blocks withdraw from each other and may be linked to the expulsion of fluids at the surface due to fracture closure (Muir-Wood, 1994).

DISCUSSION

Energy flow during frictional plastic failure can be regarded as analogous to that described for faults, but at a smaller scale. A small increment of dip slip on an optimally oriented fracture plane results in a small loss of GPE, dissipation of FE, and increase in EE_{VOL}. Similarly a local increase in horizontal stress ensures the region remains below the Mohr-Coulomb failure limit until the next episode of failure on that fracture plane.

Coseismic energy flows in the hanging wall occur in the opposite direction to those attributed to elastic rebound of the footwall. Figure 4 presents a spring-block schematic accounting for coseismic displacement, stress, and energy changes within the hanging wall for an extending crust. Dip slip of the fault block occurs when the sum of the shear components

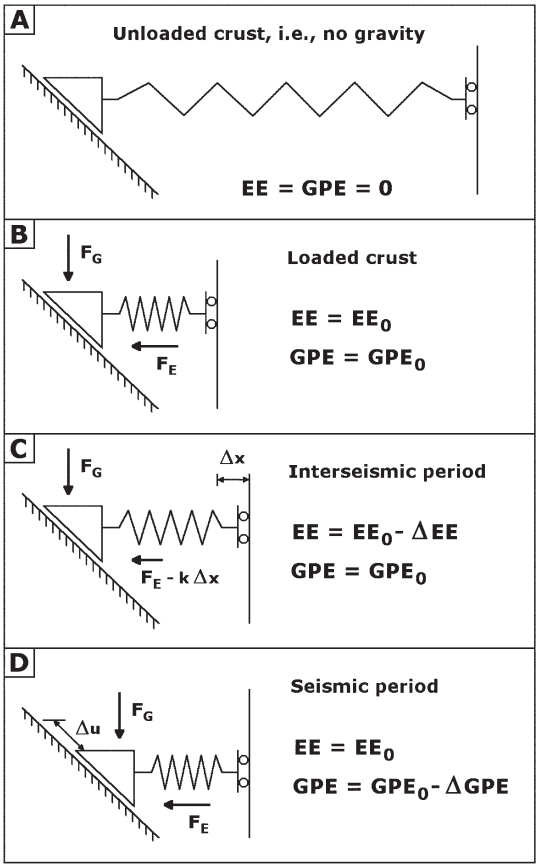

Figure 4. Spring (of stiffness k) and block model accounting for observed displacements, stress, and changes in elastic energy (EE) and gravitational potential energy (GPE) in hanging wall. A: Unloaded spring, equivalent to absence of gravity. B: Gravitational loading, F_G, compresses crust vertically and induces horizontal spring force, F_E. Sum of opposing shear components of F_G and F_E is below threshold for frictional slip. C: Increment of tectonic extension, Δx, decreases EE and reduces spring force until threshold for friction slip is exceeded. D: Dip-slip of hanging wall recompresses spring, creating EE at cost of GPE, and restores balance of forces on fault.

of the vertical lithostatic stress, a gravitational force directed down dip, and the horizontal stress, an elastic force directed up dip, exceeds the static frictional threshold. Tectonic extension, in addition to decreasing EE, causes a reduction in the up-dip shear stress, while leaving the gravitational shear component unchanged. An earthquake occurs after a sufficient reduction of the up-dip shear stress, at which time gravitational forces cause the hanging wall to shift down dip, expending GPE. Horizontal displacement of the fault block recompresses the wider crust, creating EE, and increasing the up-dip shear force on the fault such that the balance of forces is restored.

In contrast to the steady accumulation of EE required for an elastic rebound, GPE released during a collapse of the hanging wall does not accumulate during the interseismic period. Instead, GPE is always there, but is only made available to do work through the removal of elastic and frictional constraints, i.e., by imposing a material discontinuity (a fault) and then permitting slip to occur on its surface. Far-field tectonic extension is not directly responsible for loading the crust in the classical sense, i.e., by increasing its potential to do work. Rather, it alters the balance of stresses on the fault plane until failure of an already loaded crust occurs.

ACKNOWLEDGMENTS

We thank T. Wright, M. Reyners, C. Williams, and three anonymous reviewers for comments that improved the manuscript. This work is funded by the Tertiary Education Commission, New Zealand, through the Bright Futures Scheme and by an Energy Education Trust of New Zealand Doctoral Scholarship.

REFERENCES CITED

Barrientos, S.E., Stein, R.S., and Ward, S.N., 1987, Comparison of the 1959 Hebgen Lake, Montana and the 1983 Borah Peak, Idaho, earthquakes from geodetic observations: Seismological Society of America Bulletin, v. 77, p. 784–808.

Byerlee, J., 1978, Friction of rocks: Pure and Applied Geophysics, v. 116, p. 615–626, doi:10.1007/BF00876528.

Cook, N.G.W., Hoek, E., Pretorius, J.P.G., Ortlepp, W.D., and Salamon, M.D.G., 1966, Rock mechanics applied to the study of rockbursts: South African Institute of Mining and Metallurgy Journal, v. 66, p. 435–528.

Cooke, M.L., and Murphy, S., 2004, Assessing the work budget and efficiency of fault systems using mechanical models: Journal of Geophysical Research, v. 109, B10408, doi:10.1029/2004JB002968.

Cruz, L., Malinski, J., Wilson, A., Take, W.A., and Hilley, G., 2010, Erosional control of the kinematics and geometry of fold-and-thrust belts imaged in a physical and numerical sandbox: Journal of Geophysical Research, v. 115, B09404, doi:10.1029/2010JB007472.

Del Castello, M., and Cooke, M.L., 2007, Underthrusting-accretion cycle: Work budget as revealed by the boundary element method: Journal of Geophysical Research, v. 112, B12404, doi:10.1029/2007JB004997.

Ellis, S., Beavan, J., Eberhart-Phillips, D., and Stöckhert, B., 2006, Simplified models of the Alpine Fault seismic cycle: Stress transfer in the mid-crust: Geophysical Journal International, v. 166, p. 386–402, doi:10.1111/j.1365-246X.2006.02917.x.

Gudmundsson, A., 2004, Effects of Young's modulus on fault displacement: Comptes Rendus Geoscience, v. 336, p. 85–92, doi:10.1016/j.crte.2003.09.018.

Hanks, T.C., and Kanamori, H., 1979, A moment magnitude scale: Journal of Geophysical Research, v. 84, p. 2348–2350, doi:10.1029/JB084iB05p02348.

Hetland, E.A., and Hager, B.H., 2006, The effects of rheological layering on postseismic deformation: Geophysical Journal International, v. 166, p. 277–292, doi:10.1111/j.1365-246X.2006.02974.x.

Kanamori, H., 2001, Energy budget of earthquakes and seismic efficiency, *in* Teisseyre, R., and Majewski, E., eds., Earthquake thermodynamics and phase transformations in the Earth's interior: New York, Academic Press, p. 293–305.

Koukouvelas, I.K., and Doutsos, T.T., 1996, Implications of structural segmentation during earthquakes: The 1995 Egion earthquake, Gulf of Corinth, Greece: Journal of Structural Geology, v. 18, p. 1381–1388, doi:10.1016/S0191-8141(96)00071-5.

McGarr, A., 1994, Some comparisons between mining-induced and laboratory earthquakes: Pure and Applied Geophysics, v. 142, p. 467–489, doi:10.1007/BF00876051.

McKenzie, D., 1978, Active tectonics of the Alpine-Himalayan belt: The Aegean Sea and surrounding regions: Royal Astronomical Society Geophysical Journal, v. 55, p. 217–254, doi:10.1111/j.1365-246x.1978.tb04759.x.

Muir-Wood, R., 1994, Earthquakes, strain-cycling and the mobilization of fluids, *in* Parnell, J., ed., Geofluids: Origin, migration and evolution of fluids in sedimentary basins: Geological Society of London Special Publication 78, p. 85–98, doi:10.1144/GSL.SP.1994.078.01.08.

Nüchter, J.-A., and Ellis, S., 2010, Complex states of stress during the normal faulting seismic cycle: Role of midcrustal postseismic creep: Journal of Geophysical Research, v. 115, B12411, doi:10.1029/2010JB007557.

Popov, A.A., and Sobolev, S.V., 2008, SLIM3D: A tool for three-dimensional thermomechanical modeling of lithospheric deformation with elasto-visco-plastic rheology: Physics of the Earth and Planetary Interiors, v. 171, p. 55–75, doi:10.1016/j.pepi.2008.03.007.

Reid, H.F., 1911, The elastic-rebound theory of earthquakes: University of California Publications, Bulletin of the Department of Geology, v. 6, p. 413–444.

Savage, H.M., and Cooke, M.L., 2010, Unlocking the effects of friction on fault damage zones: Journal of Structural Geology, v. 32, p. 1732–1741, doi:10.1016/j.jsg.2009.08.014.

Scholz, C.H., and Engelder, J.T., 1976, The role of asperity indentation and ploughing in rock friction—I. Asperity creep and stick slip: International Journal of Rock Mechanics and Mining Sciences & Geomechanics Abstracts, v. 13, p. 149–154, doi:10.1016/0148-9062(76)90819-6.

Sibson, R.H., 1974, Frictional constraints on thrust, wrench and normal faults: Nature, v. 249, p. 542–544, doi:10.1038/249542a0.

Stewart, J.H., 1980, Regional tilt patterns of late Cenozoic basin-range fault blocks, western United States: Geological Society of America Bulletin, v. 91, p. 460–464, doi:10.1130/0016-7606(1980)91<460:RTPOLC>2.0.CO;2.

Tanimoto, T., Okamoto, T., and Terra, F., 2002, Tectonic signatures in coseismic gravitational energy change: Geophysical Journal International, v. 149, p. 490–498, doi:10.1046/j.1365-246X.2002.01662.x.

Townend, J., and Zoback, M.D., 2000, How faulting keeps the crust strong: Geology, v. 28, p. 399–402, doi:10.1130/0091-7613(2000)28<399:HFKTCS>2.0.CO;2.

Zoback, M.D., Moos, D., Mastin, L., and Anderson, R.N., 1985, Well bore breakouts and in situ stress: Journal of Geophysical Research, v. 90, p. 5523–5530, doi:10.1029/JB090iB07p05523.

Manuscript received 12 July 2011
Revised manuscript received 12 October 2011
Manuscript accepted 20 October 2011

Printed in USA